Impact of Electrolytes on Produced Water Destabilization

L. Plassard, A. Mouret, C. Nieto-Draghi, C. Dalmazzone, D. Langevin, J.-F. Argillier

Impact Of Electrolytes On Produced Water Destabilization: Plassard L.*†, Mouret A.†, Nieto-Draghi C.†, Dalmazzone C.†, Langevin D.‡, Argillier J-F.†

† IFP Energies Nouvelles, 1-4 Avenue de Bois Préau, 92852 Rueil-Malmaison, France

‡ Université Paris Saclay, Bâtiment 510, 91405 Orsay, France

***Email address: loick.plassard@gmail.com**

Abstract:

In order to increase oil recovery, new techniques were developed such as chemical Enhanced Oil Recovery (EOR). The water injected in the reservoir tend to form and stabilize emulsions of oil droplets in produced water. That makes the separation of oil from the aqueous phase more difficult. The main goal of this work is to achieve a better understanding of emulsion destabilization in presence of brine. In this work, different methods were used with emulsions and macroscopic drops to better understand oil droplets behavior. The experimental results are based on the determination of the zeta potential, the evolution of the kinetics of light transmission, the critical force of coalescence in centrifugation and on the rupture time of the aqueous thin film between an oil drop and a water/oil interface. These studies allowed to characterize the impact of salinity on emulsion destabilization. It was observed that the negative charges at the oil droplets surface, due to migration of indigenous amphiphilic species from crude oil to the interface, are reduced by the presence of salts because salts decrease the adsorption of charged natural surfactants at the oil-water interface. The electrostatic repulsion between oil droplets is thus reduced, promoting flocculation and coalescence.

I. Introduction

Nowadays the oil industry consumes a high quantity of water to produce oil, on average worldwide 3 to 5 barrels of water are necessary for each barrel of oil. This quantity of water depends on the oil field and on the maturity of production wells, the more mature the wells, the more water is used to extract the oil [1]. As water consumption is increasing, the oil industry is more concerned by water management. Produced water (PW) obtained after oil extraction contains various hazardous pollutants such as heavy metals, dissolved hydrocarbons, radioactive products or emulsified crude oil [2]. Moreover, small oil droplets can be stabilized by surface-active molecules (like asphaltenes, naphthenic acids) contained in the crude oil. PW composition is highly dependent on water composition and crude oil properties[3]. This is why PW needs to be treated, first of all, to clean the water before discharging it into the environment (ocean, river…) or to re-inject it into the production well with the aim to reduce water consumption.

There are different types of treatment in PW management: physical, chemical and biological [4–7]. These techniques aim to remove pollutants from PW, especially dispersed particles and oil droplets as they pose issues during reinjection in the environment or in the wells. Currently, several regulations restrict the concentration of crude oil dispersed in the discharge water to 30-40 ppm. However, in order to re-inject the water into the production wells, the concentration of dispersed droplets is even lower, typically less than 5 ppm[8]. One of the main methods used in water treatment facilities is hydrocyclone because of its efficiency in removing pollutants at a large scale [9]. This efficiency is strongly dependent on the oil droplet size and the difference in density between oil and water, which will control the separation rate[10,11].

Oil-water separation is accelerated in hydrocyclones thanks to centrifugation. The density of oily and aqueous phases are almost similar and the smallest oil droplets are not easily removed from the PW. For the purpose of increasing the efficiency of oil droplet removal, several methods are usually combined [7].

For oil droplets in water, electrostatic forces may become stronger than hydrodynamic forces when the droplets are close enough. Films may form between them, which drainage is impacted by the Gibbs interfacial elasticity, for example a rigid interface slows down the coalescence process [12]. A model for the drainage of thin liquid films bounded by viscoelastic interfaces was developed by Tambe and Sharma in order to better understand this complex process [13].

Crude oil is composed of a variety of species including surface-active species. These species alter the coalescence of oil droplets in PW. Note that PWs are very dilute oil-in-water emulsions. Most of the investigations carried out with crude oils concerning the coalescence and/or stability of emulsions were done with water-in-oil emulsions [14–16]. However, studies of oil in water emulsions were performed in relation with crude oil transportation and more recently with PWs [17–20].

The stability of PW emulsions depends on both water and oil composition [3,21]. The water phase may contain salts, surfactants and polymers which role is important. The description of the role of salt is the aim of the present paper, the role of surfactant and polymers will be described in a forthcoming paper. Crude oils are mixtures of many different components which also affect PW stability. When crude oil comes into contact with water, surface-active molecules diffuse through the bulk oil phase and reach the oil/water interface. This adsorption at the interface impacts the coalescence of the crude

oil droplets by reducing the interfacial tension and forming a viscoelastic interface. The interfacial properties evolve over long times, a phenomenon called interfacial ageing [16].

Among the components of a crude oil, asphaltenes are the heaviest (in terms of molecular weight) and one of the most polar compounds [22]. Asphaltenes can be found in crude oils, especially heavy crude oils or bitumen and are usually aggregated within the bulk oil. Asphaltenes tend to adsorb at the oil/water interfaces [23,24]. These species are considered as natural oil surfactants but even today their chemical structure is not yet well known [25]. The asphaltenes are responsible for the high viscosity of crude oil (that poses transportation problems) and for the stabilization of water-in-oil emulsions formed just after oil extraction (that impacts oil/water separation) [26,27]. Furthermore, the pH of water changes after contact between crude oil and water and adsorption of these species at the oil/water interface[28]. This variation in the pH is due to the transfer of crude oil species such as naphthenic acids into water [29]. Naphthenic acids (carboxylic, aromatic and acyclic acids of crude oil) ionize at the interface and lower the interfacial tension between brine and crude oil [30].

In this context, the impact of the presence of salts (composition and concentration) is not negligible. Lashkarbolooki et al. reported a "salting-in" or "salting-out" effect with PWs, corresponding to a change in the distribution of surface-active molecules (such as asphaltenes and resins from crude oil) at the oil/water interface and affecting the IFT between brine and crude oil [31]. Regarding the flotation process, Chakibi et al. reported that the presence of salt in the PW reduces the electrostatic repulsion between oil droplets and air bubbles, which improves the attachment of droplets to bubbles and facilitates the rupture of the thin aqueous films formed between them [20]. Other studies are focused on the effect of the presence of different inorganic ions (Na^+, Ca^{2+}, Mg^{2+}, K^+, SO_4^{2-}, Cl^-, HCO_3^-) in water on the properties of oil-water interfaces [32–36]. Recently, Wang et al. showed that salts in the aqueous phase slow down the coalescence of toluene droplets stabilized by stearic acid [37]. They attributed this effect to the specific adsorption of ions at the oil-water interface, by analogy with the suppression of coalescence of bubbles in water when salt is added. This phenomenon is opposite to what was reported by Chakibi et al. for the coalescence of air bubbles at the interface between brine and crude oils. In the later work, it was shown that the zeta potential of the oil-water interfaces increases when salt is added, whereas this potential remains constant when pure oils such as dodecane are used. It therefore appears that the role of the indigenous surfactants in crude oil is important. The impact of salts in solution on the oil/water interfaces needs therefore to be investigated further, particularly for crude oils containing surface-active species.

Emulsion stability also depends on the ionic strength which determines the Debye length, comparable to the equilibrium thickness of the films formed between two oil drops. As the ionic strength increases, the film thickness decreases and coalescence is easier. Finally, emulsion stability also depends on the rheological properties of the layer of surface-active substances adsorbed at the drop surfaces. When the layer composition changes, the surface rheology may change as well and coalescence affected. It is therefore not easy to find out which phenomenon plays the leading role.

The aim of the present work is to investigate the impact of water-soluble ions (NaCl and $CaCl_2$) on the coalescence of crude oil droplets leading to the separation of oil and water. For this purpose, various complementary experimental techniques were used and the behavior of oil drops at different sizes was investigated as a function of water salinity. We studied the coalescence of emulsion drops under the influence of a centrifugal force and the coalescence of larger individual drops with a flat interface.

The coalescence process involves the rupture of thin liquid films formed between either a drop and a flat interface, or between two drops. The film thickness is governed by surface forces, which are the same, and surface rheological properties which are also the same. It is therefore widely admitted that coalescence proceeds in the same way in the two types of systems and numerous confirmations can be found in the literature[12].

In this paper, section II presents the methods used to prepare and analyze the PW, section III reports the results obtained and section IV outlines the main conclusions of this work.

II. Experimental section

All experiments were performed at room temperature (20°C) and atmospheric pressure.

a. Brine

Two different salts, sodium chloride (Merck) and calcium chloride (Merck of analytical grade with purity higher than 99.9%) were used without other specific treatment. The brine was prepared by dissolving the salt in demineralized water. In order to compare results obtained with both salts, brines with the same ionic strengths I were used; I is given by the following equation:

$$I = \frac{1}{2}\sum_{i}\left(C_i * z_i^2\right) \quad \textbf{(1)}$$

With C_i the molar concentration of ions in water (mol/L) and z_i the valence of ions.

b. Crude Oil

Except when noted, the oil sample used for this study is a heavy crude oil diluted in xylene (purity > 99%, VWR) with a dilution factor of 2 in weight. This diluted crude oil had a viscosity of 5.1 mPa.s (in ambient conditions), an API° of 22.9 and an asphaltene content of 4.2 wt% in the SARA cut. This dilution was necessary to prepare a concentrated oil-in-water emulsion because it reduced the viscosity of oil and allowed better emulsification of oil into water.

For information, the initial heavy crude oil used to prepare the diluted oil sample has a viscosity of 15.5 Pa.s at 20°C and its characteristics are shown in Table 1.

Table 1: characteristics of the crude oil.

Density at 15°C (kg/m^3)	969.7
API°	14.4
Total acid number (mg KOH/g)	2.04
Elements analysis (%w/w)	
C	86.6
H	11.5
N	0.52
O	0.49
S	0.43
SARA cut at T>344°C (%w/w)	

Saturates	26.9
Aromatics	32.4
Resins	27.9
Asphaltenes (C_7 extraction)	8.3

c. Synthetic produced water

The aim of this fabrication protocol is to obtain stable synthetic PW with oil droplets of size similar to that of oil droplets observed during the treatment of PW during oil recovery.

In a first step, a concentrated "mother" emulsion is prepared. Its aqueous phase contains 1 wt% of a nonionic surfactant, Triton X-405 (Sigma-Aldrich) to stabilize the oil droplets, and 0.1 wt% of a polymer HPAM 3630S (SNF Floeger) to increase the viscosity of water ($\eta_{aqueous\ phase}$ = 31.2 mPa.s), with a thinning fluid behavior, facilitating emulsification. In addition to Triton X-405 and HPAM 3630S, this aqueous phase also contains 7.5 g/L (128 mM) of NaCl.

The diluted crude oil is then dispersed in the aqueous phase using an Ultra-Turrax disperser to form a concentrated oil-in-water emulsion (70% wt% of oil). The Ultra-Turrax disperser was run at 5000 rpm for 2 min during oil introduction and then at 12 000 rpm for 5 min.

A Mastersizer 2000 laser granulometer (Malvern Instruments) was used to measure the diameter of the oil droplets in the mother emulsion. The analyzed samples were diluted with purified water and their size distribution is shown in Figure 1. The peak at 1.4 µm corresponds to small droplets obtained during the fragmentation process using the Ultra-Turrax disperser [38].

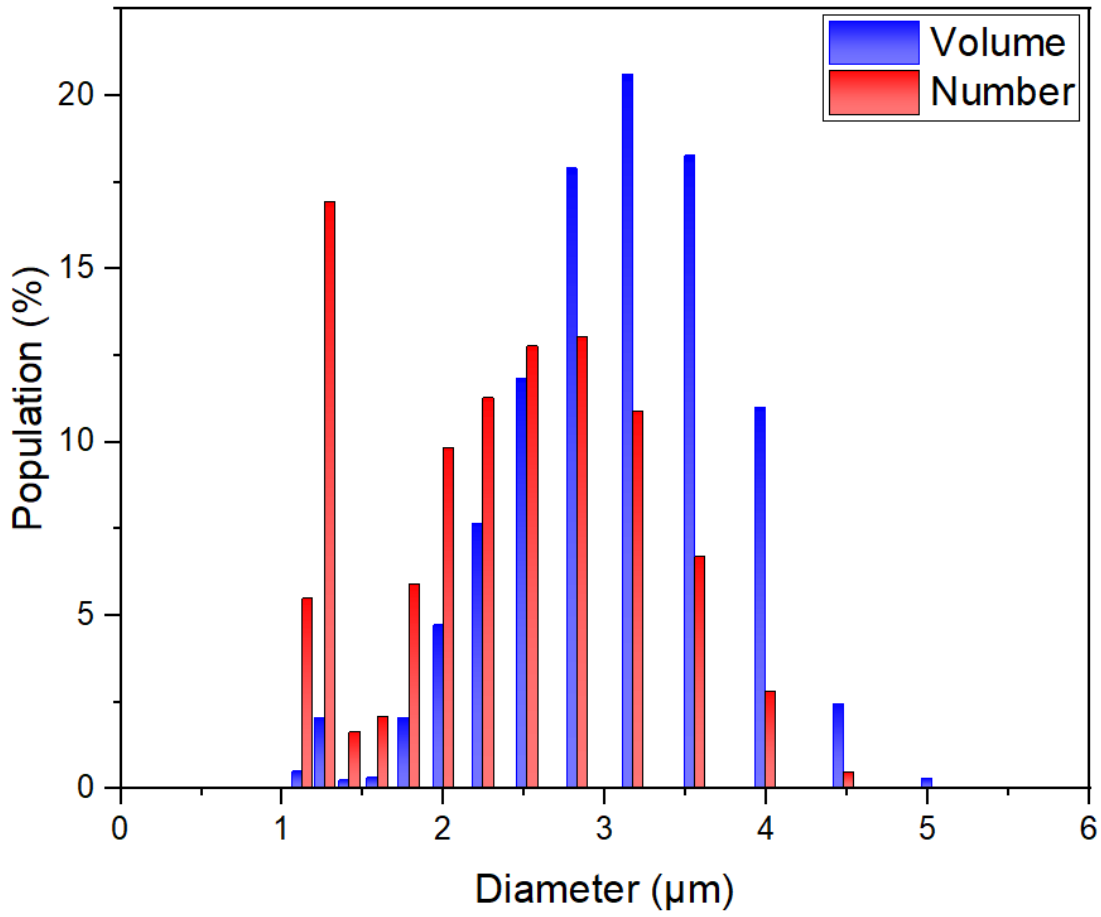

Figure 1: Granulometry of the oil droplets of a synthetic PW in number and volume obtained by laser granulometry.

This concentrated mother emulsion is then diluted in brine to a final oil concentration equal to 1000 mg/kg (unless stated otherwise). The mother emulsions were very stable and were diluted typically one week after preparation. The diluted emulsions were used immediately after preparation.

Dilution was performed with brines of different salinities, containing either NaCl or $CaCl_2$. The dispersion of oil droplets was performed by manual agitation. Note that these brines do not contain either surfactant or polymer; the only surfactant and polymer left in the PW comes from the mother emulsion and is very small due to the large degree of dilution (factor ~ 1000). There is also residual salt coming from the mother emulsion. These residual amounts are 2.25 mg/kg of NaCl, 3 mg/kg Triton and 0.3 mg/kg HPAM. The residual salt concentration is negligible compared to the salt concentration in the brines used for the dilution. The residual surfactant is much smaller than the critical micellar concentration (2.44 g/kg at 25°C). In order to evaluate its possible role, we measured the interfacial tension between the diluted crude oil and the brine (7.5 g/L NaCl) without surfactant and with the residual surfactant: we found 24.8 ± 0.5 mN/m and 18.0 ± 0.7 mN/m respectively. The decrease in IFT produced by the surfactant will have an impact on the formation of the emulsion by generating finer drops, which is what is desired for the mother emulsion. The impact on the coalescence after centrifugation should be more limited, as discussed later onThe presence of residual polymer (after dilution) does not affect the rheological behavior of PW (as measured with a rheometer DHR-3, TA Instrument): the viscosity of the PW is the same as that of brine without polymer. Interfacial tension measurements showed that the polymer does not adsorb at the oil-water interface. For instance the

tension with residual polymer is 24.4 ± 1 mN/m, equal to that without polymer within error bars. Similarly, there is no synergistic effect with the surfactant, because the tension with both residual polymer and surfactant is 17.7 ± 0.3 mN/m, equal to that without polymer within error bars. Hence this polymer cannot affect the properties of the interfacial layers either and for instance induce drop flocculation.

We will present later optical microscopy determinations of the droplet size in the PWs. The average droplet size is the same than that obtained from granulometry, showing that the size of the oil droplets was not influenced by dilution with water without added salt.

Images of the PW were taken with an optical microscope (BX51 from OLYMPUS). One can see on the images that oil droplets are not flocculated: no aggregates are visible in the images (see Figure 2). This confirms the existence of repulsive forces between the drops.

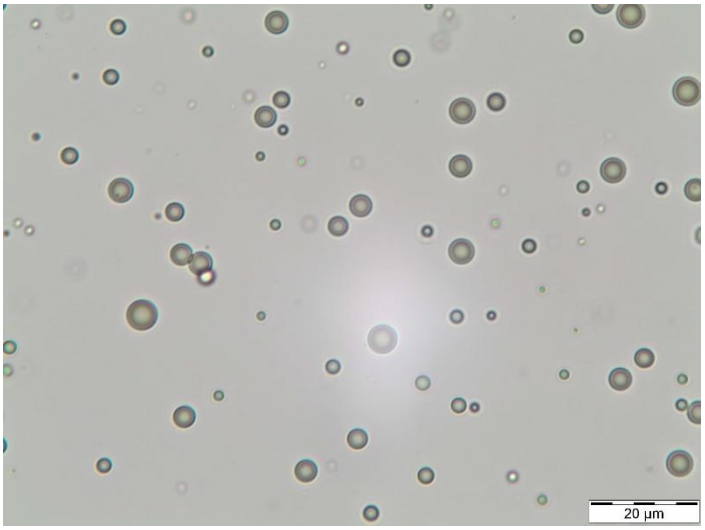

Figure 2: An optical microscopy image of freshly prepared PW at 1000 mg/kg diluted oil. Scale = 20 µm (dotted line).

d. Monitoring of emulsion creaming

Creaming of the PW was first monitored using a Turbiscan device (Formulaction) at room temperature. This equipment allows measuring over time the light transmission and backscattering of the liquid samples placed in vertical tubes. Here the PWs contains small amounts of oil, hence the transmission is used to follow their creaming (backscattering is rather used for the analysis of opaque and concentrated media). Figure 3 shows a typical example of the evolution of the PW transmission.

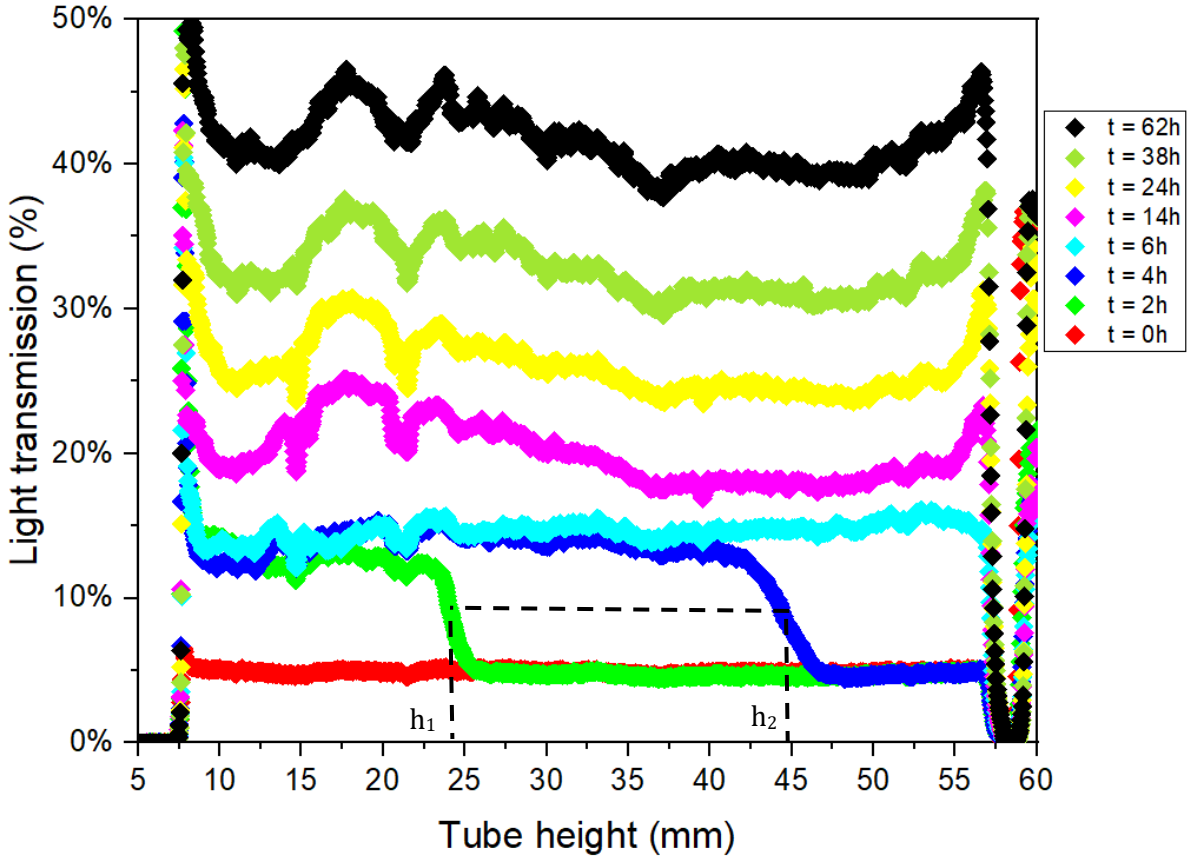

Figure 3: Typical evolution of the transmission over time of a PW with 0.06 g/L of NaCl (t = 0h corresponds to 5 min after PW preparation). The dotted lines show the characteristic height of the creaming front at different times (Turbiscan).

In this graph, we first note that the transmission is the same along the tube height (within about 5%) over the whole sample at t = 0 s. Secondly, we observe two steps during the oil droplets creaming. The first step is a creaming front visible at t = 2h and 4h and the second step is a homogeneous increase of the transmission over the whole sample (from t = 6h). The first step is due to the creaming of the largest oil droplets contained in the PW. By measuring the height of the tube from the center of the creaming front at two different times, it is possible to calculate the creaming speed of the drops.

$$v = \frac{d}{t} = \frac{h_2 - h_1}{t_2 - t_1} = 2.8\ \mu m/s \qquad \textbf{(2)}$$

The creaming velocity of single droplets is given by the Stokes equation:

$$v_{Stokes} = \frac{1}{18} \times \frac{\Delta\rho \times g \times d^2}{\eta} \qquad \textbf{(3)}$$

where $\Delta\rho$ is the difference of density between the continuous and the dispersed phase (88.16 kg/m^3), g is the standard acceleration due to gravity (equal to 9.81 m/s^2), d is the diameter of the droplet and η is the viscosity of the continuous phase.

Using this equation, the diameter of the oil drops responsible for this creaming front is found to be 7 μm. This diameter is about twice that of the largest drops, measured by laser granulometry. This growth could be due to early flocculation or coalescence of oil droplets.

The second step does not reveal the existence of a well-defined size of the droplets that cream after the initial ones. This is in fact consistent with the polydispersity of oil droplets found by granulometry. Taking for instance a collection of droplets with diameters between d and 2d, their creaming velocity will differ by a factor 4 and if the smallest have reached a height of 10 mm in the tube, the largest will have reached a height of 40 mm, meaning that a regular increase of the transmission should be observed rather than a well-defined front. The timescale of the creaming is also consistent with the average droplet size: the Stokes velocity of droplets with a diameter of 3 μm is 0.5 μm/s, and the time needed to reach the height of 50 mm is 24 hours.

The creaming of oil droplets is relatively long, it is necessary to wait 62 hours after the preparation of the PWs to reach a transmission on the whole sample of about 40%. This is why we chose not to use the Turbiscan to follow the evolution of the light transmission over time but a LUMiSizer (LUM GmbH) which allows accelerating the creaming kinetics of the oil droplets by centrifuging the PW.

The emulsion stability of freshly prepared synthetic PW subjected to centrifugation was monitored with the LUMiSizer. A rectangular glass cell with a thickness of 1 cm was filled with synthetic PW, then this cell was placed in the LUMiSizer. In order to determine the clarification time and the kinetics of light transmission evolution, the synthetic PW was subjected to the centrifugation of 120 g (equal to an angular velocity of 1000 rpm) for 4h at 20°C. During centrifugation, the LUMiSizer measured the light transmission (λ = 865 nm) of PW every 30 s over the entire sample (one detector every 14 μm). An example of the evolution of light transmission over time of a synthetic PW is shown in Figure 4, each curve representing the transmission of the whole sample at a given moment.

The timescales are reduced, but consistent with those measured with the Turbiscan: an acceleration of 120 g increases the creaming velocity by a factor 120, and a typical time of 20’ to reach a transmission of 50% in the LUMiSizer translates into a time of 40h in the Turbiscan, consistent with the observations (see Figures 3 and 4). The LUMiSizer observations are also consistent with the creaming of droplets of average diameter of 3 μm.

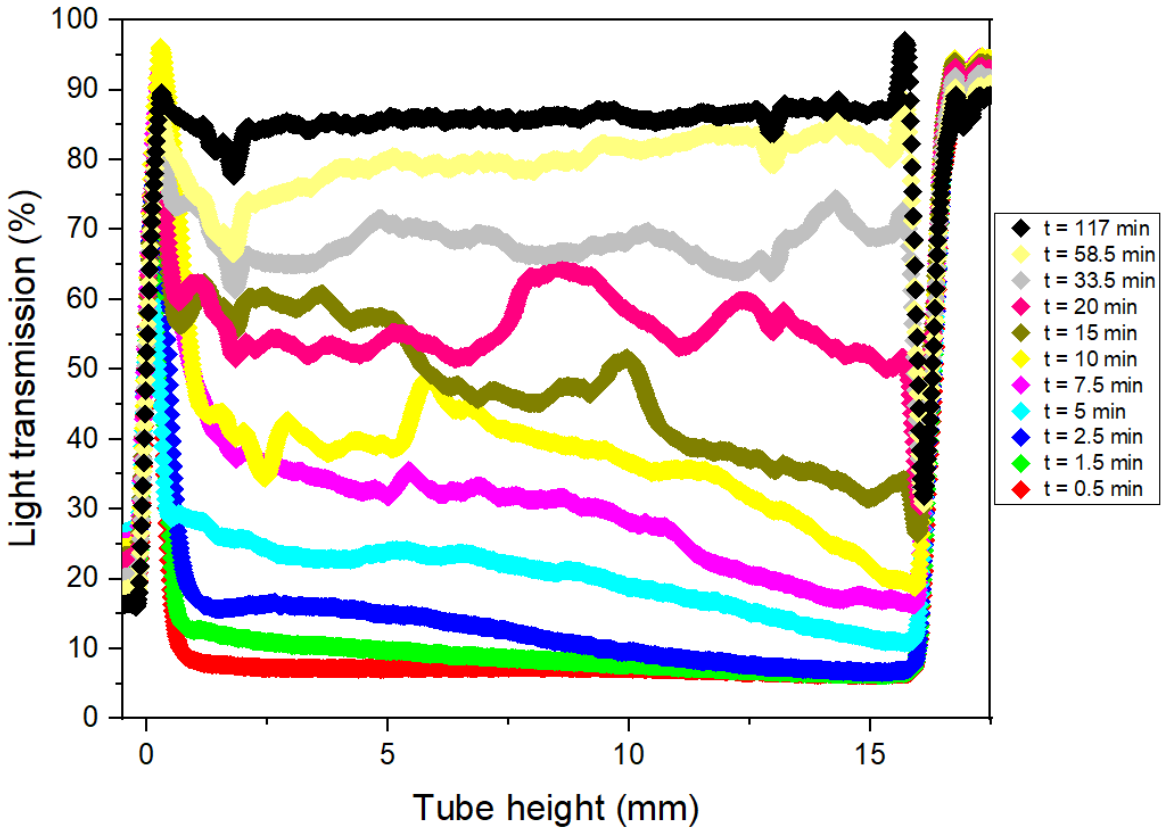

Figure 4: Example of the evolution of the light transmission of a synthetic PW over time as a function of the height of the cell (t = 0h equals to 5 min after PW preparation) (LUMiSizer).

Note that the two steps observed during the PW creaming in the Turbiscan are less distinct in the LUMiSizer. Fluctuations in light transmission appear after a certain time and possibly arise from the adhesion of some oil droplets on the walls of the glass cell, as observed after centrifugation.

The results obtained with the LUMiSizer allow the determination of a clarification time as well as the kinetics of light transmission evolution. In order to determine these parameters, we followed the light transmission of the PW over time at a given point in the centrifuge tube, at a tube height of 12.5 mm over a total height of about 15 mm. We chose this particular point because the dispersion of the measured light transmission is less close to the top of the sample. An example of the evolution of transmission over time at this point in the sample is shown in Figure 5.

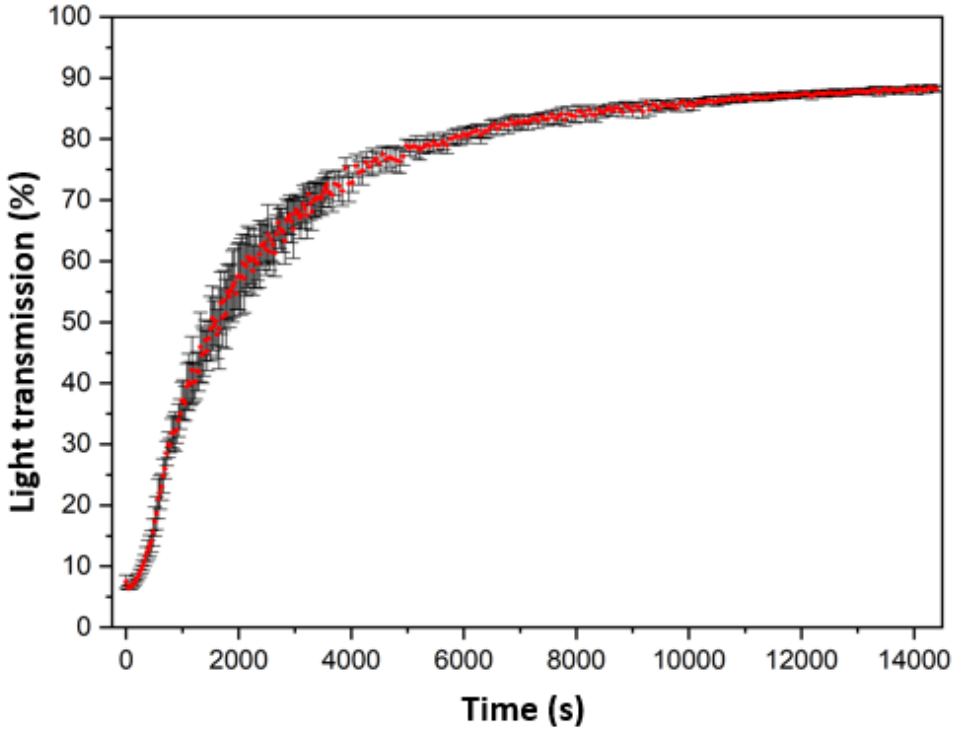

Figure 5: Evolution of the transmission over time of a production water at 1000 mg/kg of diluted crude oil at a tube height of 12.5 mm (LUMiSizer).

The evolution of the transmission is sigmoidal, i.e., the transmission increases sharply at short times (t < 3000s) and then more slowly until it reaches the maximum transmission of about 90% (which corresponds to the transmission of water). We fitted these curves using the following empirical equation:

$$T = T_{final} + \frac{T_{initial} - T_{final}}{1 + \left({}^{t}/_{t_0}\right)^{p}} \quad \textbf{(5)}$$

where T is the transmission (%), T_{final} the transmission at the end of the centrifugation (%), $T_{initial}$ the initial transmission (%), t the time (s), t_0 the transmission half-lifetime (s) and p an exponent related to the sharpness of the intermediate increase.

This fitting allows determining the clarification time and the kinetics of the evolution of the light transmission. The clarification time is defined as the time required to reach a transmission greater than or equal to 50%.

e. Critical force determination

A freshly prepared synthetic PW was observed with the microscope before centrifugation to check for the initial droplet size. The centrifugation was performed during one hour at different rotational speeds with the centrifuge RC5C (SORVALL). A concentrated emulsion separates from water at the top of the tube; this emulsion will be called “cream” in the following. The critical force for oil drop

coalescence was determined by withdrawing the cream and observing it under an optical microscope. Examples of images are shown in the Appendix. The critical force corresponds to the force required to break the aqueous thin film between the oil droplets to form a macroscopic oil film. The aim of this experiment was to link the centrifugal force applied to the energy barrier to be overcome, in order to obtain a macroscopic oil film after coalescence of oil droplets. In these experiments, the diluted crude oil concentration in synthetic PWs was 5000 mg/kg instead of 1000 mg/kg to obtain a larger volume of cream and to facilitate sampling.

We calculated the osmotic pressure (Π) in the cream with the following relationship:

$$\Pi = \Delta\rho \times \omega^2 \times r_1 \times \Delta r \quad \textbf{(6)}$$

In this equation, $\Delta\rho$ corresponds to the density difference between the oil and aqueous phases, ω to the rotational speed, r_1 to the distance between the rotational axis and the air-emulsion interface and Δr to the cream thickness. The details of this calculation are reported in the Appendix.

f. Zeta Potential Measurement

The zeta potential (ZP) of the freshly prepared synthetic PW was measured using a ZetaSizer (NANO-ZS, Malvern Instruments). After filling the electrophoresis cell with synthetic PW, an external electric field was applied to the emulsion which causes the oil droplets to move. The instrument allows calculating the electrophoretic mobility which is related to the zeta potential.

g. Crude oil drop coalescence measurement

The phenomenon of coalescence occurs in PW and leads to the growth of oil droplets. During this process, oil droplets approach each other and an aqueous thin film is formed between them [39,40]. After that, this aqueous film is drained until it breaks and oil droplets merge [39,40]. The film can have different shapes, if there are few surfactants at the interfaces, the surface of droplets is deformed (into dimples or other shapes) and coalescence occurs in the thinnest film regions [41]. Films do not form between small droplets (radius of about few micrometers) because the Laplace pressure inside the droplets is high [42] unless the interfaces repel each other and the repulsion overcomes the Laplace pressure [43]. The coalescence time is the sum of draining time and rupture time [44]. Molecular forces between oil droplets manifest themselves in general when the distance between droplets becomes of the order of 100 nm [45].

In contrast to the other experiments where a produced water, i.e. an oil-in-water emulsion, was studied, diluted crude oil drops (with an oil fraction of 90 wt%) of millimetric size were used. We used a setup built by Chakibi et al to characterize coalescence in an air/water/oil system [20]. The setup was implemented for the measurement of the rupture time between a drop and a planar oil/water interface. A glass cube was filled with brine, then a drop of diluted crude oil of diameter 6 ± 0.4 mm was formed in the brine with a syringe and a curved needle (0.9 mm diameter). The bottom of this needle was fixed to the bottom of the glass cube and the volume of brine was constant in order to maintain the same distance (1.6 cm) between the oil drop and the oil/water interface. With the aim to limit the vibration of the interface and to avoid lateral deviations of oil drops along the interface, a 35 mm diameter hydrophobic Teflon ring was placed at the interface, creating a convex interface. A layer

of diluted crude oil was then inserted inside the ring. Figure 6 shows a schematic diagram of this technique.

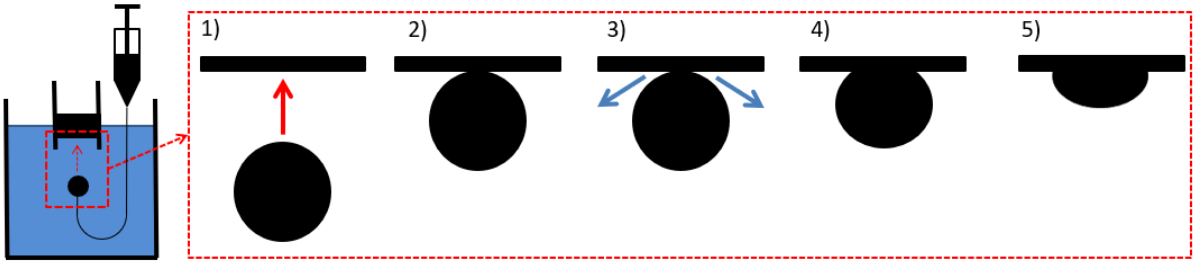

Figure 6: Schematic diagram of the coalescence measurement of an oil drop with a "plane" water/oil interface. 1) Formation/Ascension of the drop; 2) Contact between the interface and the drop; 3) Drainage of the aqueous thin film; 4) Rupture of the aqueous thin film; 5) Spreading of the drop.

Oil drops were formed in the brine and after 1-6 minutes were left to ascend towards the interface, at room temperature. An i-SPEED 2 camera (OLYMPUS) was used to record the rise and coalescence of oil drops, with a frame rate of 100 frames per second; the accuracy on the rupture time is ± 10 ms. The rupture time was set as the time elapsed between the first contact between the oil drop and the oil/water interface and the rupture of the aqueous thin film. In order to facilitate the formation of the oil drops, the crude oil was diluted with xylene with a mixture of 90%wt crude oil and 10%wt xylene which is different from the dilution factor of the diluted crude oil contained in the PWs.

III. Results and Discussion

a. Zeta potential (ZP)

An important parameter in the process of oil droplet coalescence in PW is the zeta potential (ZP). As explained in the Introduction, the contact and fusion between two oil droplets depend on the stability against rupture of the aqueous thin film, which is formed when the oil droplets approach each other. This stability is related to the interaction between oil/water interfaces, with the ZP representing the electrostatic forces in the studied system. When the ZP is very small, attractive van der Waals forces may dominate and lead to film rupture. The ZP of diluted and non-diluted crude oil droplets in PW were measured for a monovalent (NaCl) and a divalent ($CaCl_2$) salt and the results are shown in Figure 7.

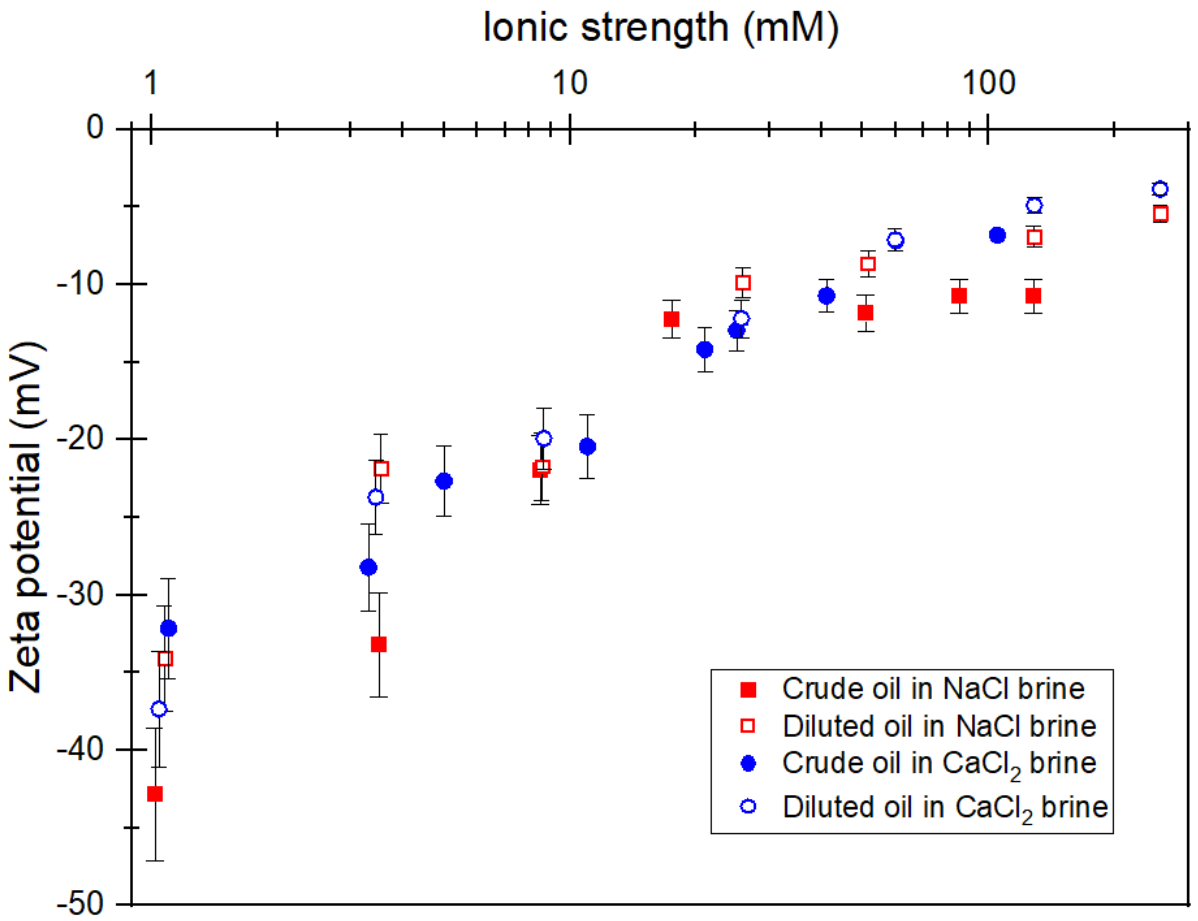

Figure 7: Zeta Potential of crude oil droplets in brines of different salinities: NaCl (red squares) and $CaCl_2$ (blue circles). Zeta potential of diluted crude oil (50%wt of crude oil in xylene) droplets in brines of different salinities: NaCl (empty red squares) and $CaCl_2$ (empty blue circles).

These measurements show that the surface charge of the oil droplets in the PW is negative as expected for this kind of emulsions [20]. This is largely due to the ionization of the polar chemical species of oil (naphthenic acids, asphaltenes...). This ionization leads to a transfer of these chemical species from the oil phase to the water phase, some species remaining adsorbed at the water/oil interface [29]. The zeta potential does not depend on the degree of dilution of the crude oil in the drops within error bars. The absolute value of ZP decreases when the ionic strength increases for the two salts studied. This is due to a modification of the species adsorbed at the water/oil interfaces [46]. Chakibi et al. observed the

same trends for ZP measurements of droplets of another heavy crude oil dispersed in brines (NaCl and $CaCl_2$) [20].

In addition, Chakibi et al. noted that the ZP of dodecane droplets dispersed in brine (NaCl) and stabilized by a non-ionic surfactant is not altered by ionic strength [20]. This shows that the effect of electrolytes on the zeta potential of crude oil droplets is not a shielding effect of surface charges. The ionic strength modifies the partition coefficient of ionizable species between the oil and water phases and changes the nature of molecules adsorbed at the interfaces.

In order to check if the electrostatic repulsion evolves over time, we measured the ZP of oil droplets at different salinities. The first ZP measurement was made shortly after the preparation of the production water (less than 5 min, considered as zero in Figure 8). These ZP measurements are shown in Figure 8.

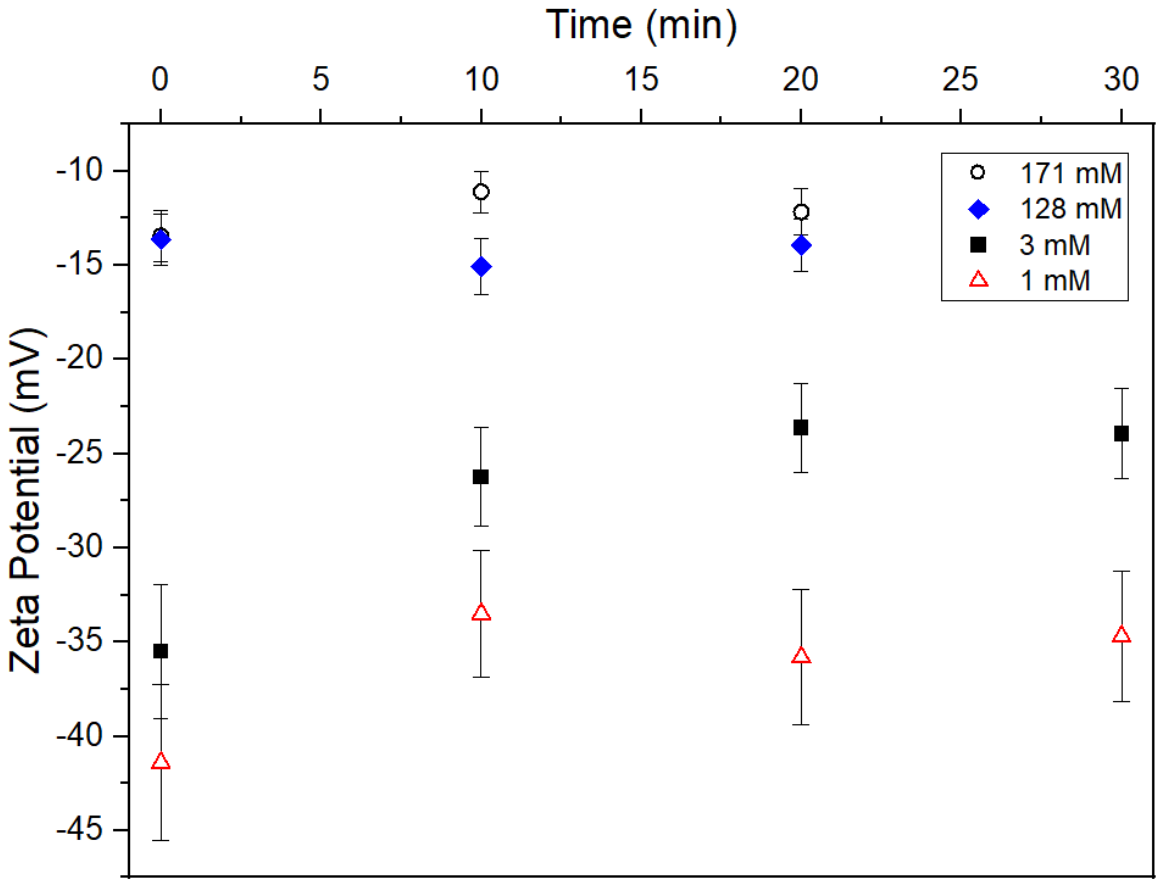

Figure 8: Zeta potential of non-diluted crude oil droplets in brines based of NaCl as function of time, at different salinities.

At low salinity, the absolute values of ZP tend to decrease during the first 10 minutes after the preparation of the production water and then stabilize. It is assumed that ZP variations are due to the modification/reorganization of natural crude surfactants adsorbed at the surface of the oil droplets. It should be noted that the interfacial changes seem to be faster at high salinity: equilibrium is reached in less than 5 min.

b. Emulsion destabilisation

i. Produced water destabilisation

According to Stokes' law (equation 3), the creaming velocity of dilute emulsions is directly related to the droplet size. The method used allows determining the kinetics of light transmission evolution and the clarification times by following the evolution of the light transmission of the synthetic PW subjected to centrifugation over time.

Clarification time

A clarification time is defined as the time required to reach a transmission higher or equal to 50%. This time is used to characterize the oil droplets creaming determined with the transmission curves fitted with equation 5. The clarification times are plotted as a function of the ionic strength for the two salts studied in Figure 9.

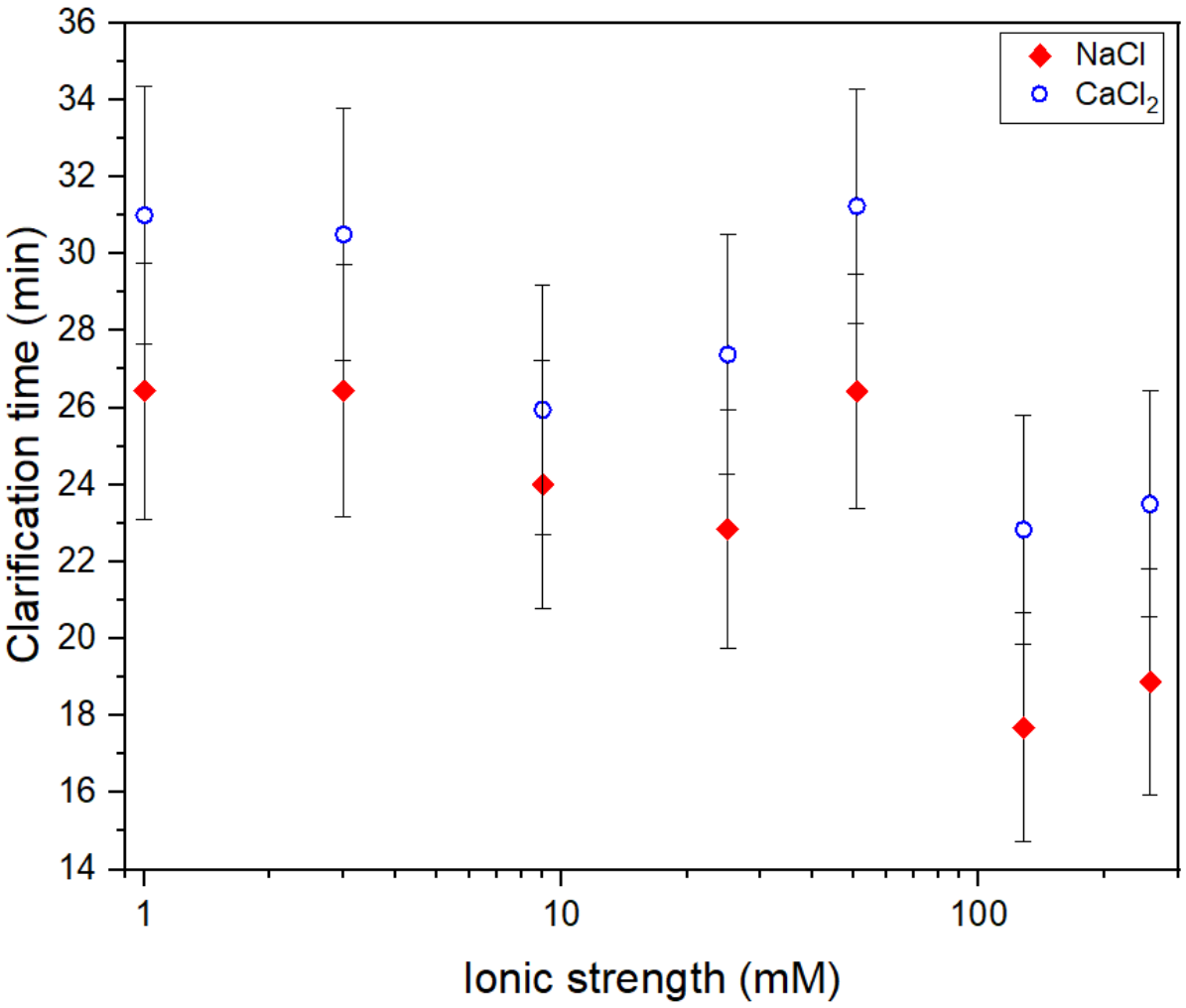

Figure 9: Clarification time as a function of the ionic strength of produced water with brines with NaCl (red diamonds) and $CaCl_2$ (empty blue circles).

We find that the clarification time decreases as the ionic strength of the brines used to prepare the PW increases. This trend is present for both salts, but the clarification times are slightly higher in the

presence of $CaCl_2$ than in the presence of NaCl with equal ionic strength. These results show that the salts accelerate the creaming of the oil droplets.

Kinetics of light transmission evolution

Figure 10 shows the slope of the curve at the inflexion point that we chose to use to characterize the time evolution of light transmission and to quantify the impact of salt on the creaming.

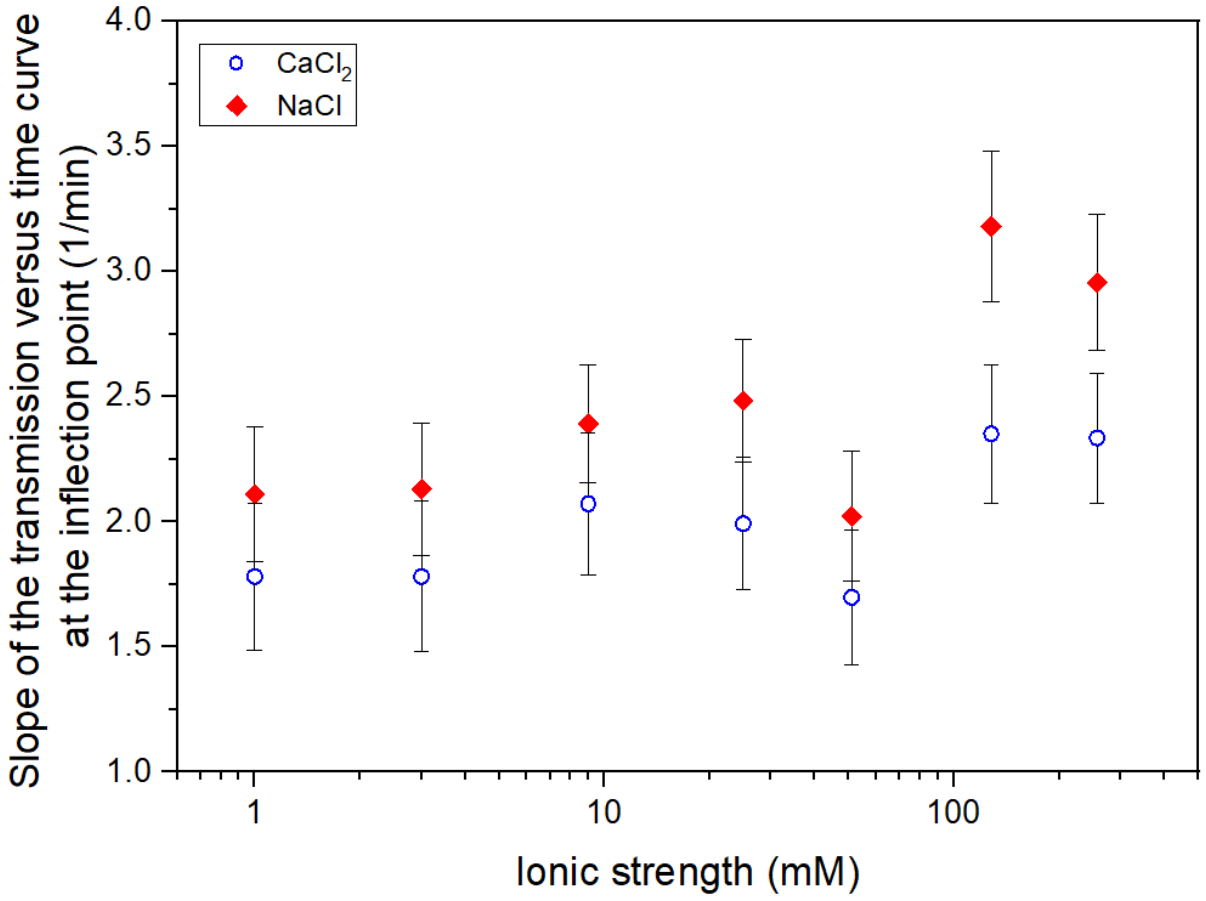

Figure 10: Slopes of the fitted curves of time evolution of light transmission evolution as a function of the ionic strength of produced water with brines with NaCl (red diamonds) and $CaCl_2$ (empty blue circles).

The results show qualitatively that the higher the ionic strength, the faster the kinetics of evolution of the transmission is for both salts. We see the same trends as observed with the clarification times, e.g. NaCl has a greater impact than $CaCl_2$ because the kinetics is faster. This trend could be due to a specific affinity between water-soluble ions and indigenous surfactants from the crude oil. However, the difference between the salts is within the uncertainty of the results. As expected, there is a good correlation between the clarification times and the time evolution of the transmission.

Faster clarification means that the oil droplets creaming is faster. Since everything else is constant, this acceleration can only be due to an increase in the size of the objects.

It is well known that in crude oil emulsions, the oil droplets are stabilized through electrostatic repulsion due to the adsorption of the native surface-active molecules of the crude oil at the water/oil interfaces. Zeta potential measurements show that the presence of salt in the aqueous phase reduces

the electrostatic repulsion, allowing oil droplets to come closer together and leading to flocculation and/or coalescence and thus increasing the size of the dispersed objects.

To confirm this hypothesis, we observed by optical microscopy oil droplets in the PW, before and after centrifugation at 120 g (equal to that applied in the LUMiSizer). Figure 11 shows the images of the freshly prepared PW obtained with a light microscope.

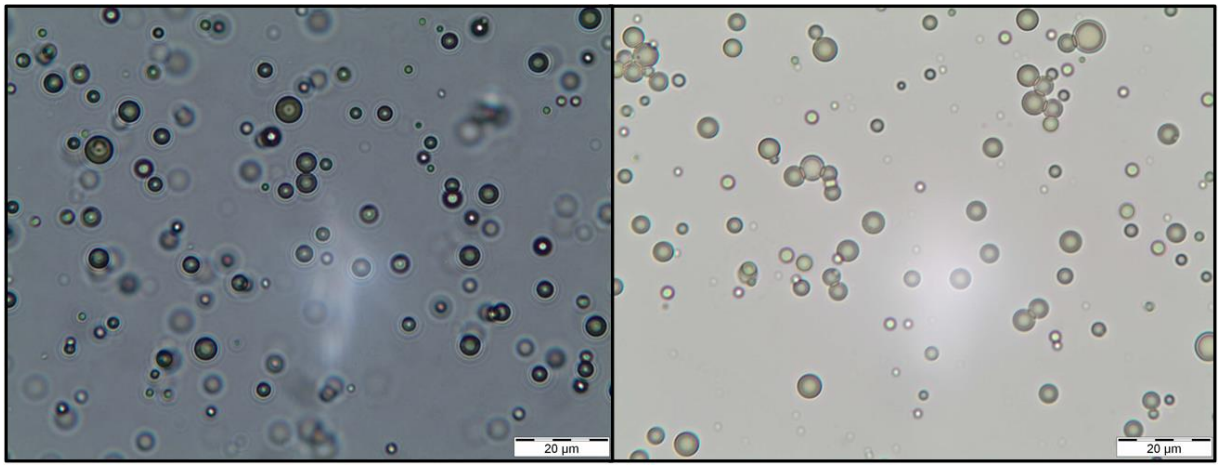

Figure 11: Optical microscopy images of PW at 5000 mg/kg diluted oil before centrifugation for a NaCl concentration of 0.06 g/L (at left) and 7.5 g/L (at right). Scale = 20 µm (dashed line).

Figure 11 shows that before centrifugation, flocculation of the oil droplets is not observed. This is the case for all salinities studied and for the two salts. Figure 12 shows the image of a cream after centrifugation.

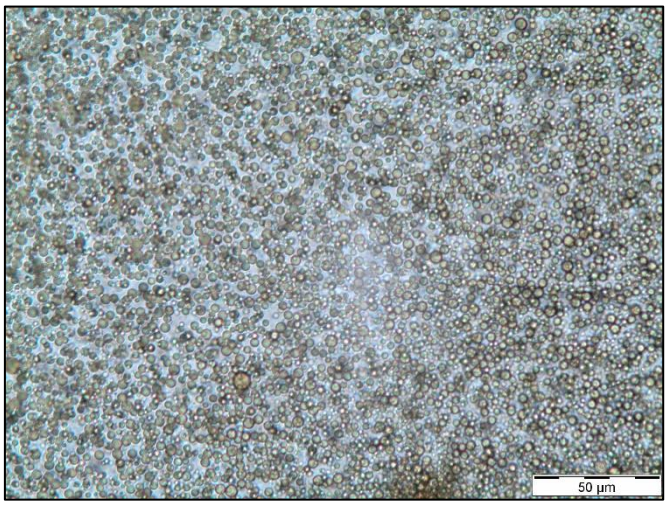

Figure 12: Optical microscopy images of PW at 5000 mg/kg diluted oil after one hour of centrifugation at 6300g for a NaCl concentration of 1.5 g/L. Scale = 50 µm (dashed line).

We have then used the images to determine the droplet size before and after centrifugation for different salt concentrations. We first opted for a measurement followed by image processing to take into account as many droplets as possible. However, the images obtained do not allow automatized treatment because the contrast between the droplets and the continuous phase is not sufficient to correctly measure the size of the oil droplets. The analysis was finally performed manually. The very small droplets (diameter below about 2 µm) are difficult to analyse. Since they are not too numerous

(see figure 1), , we chose to measure only the largest oil droplets (d > 2.5 µm). The distinction between single droplets from flocculated ones is meaningless in creams, where all the droplets can be considered as flocculated. Therefore, the results shown in Figure 13 represent the evolution of the drop size due to coalescence.

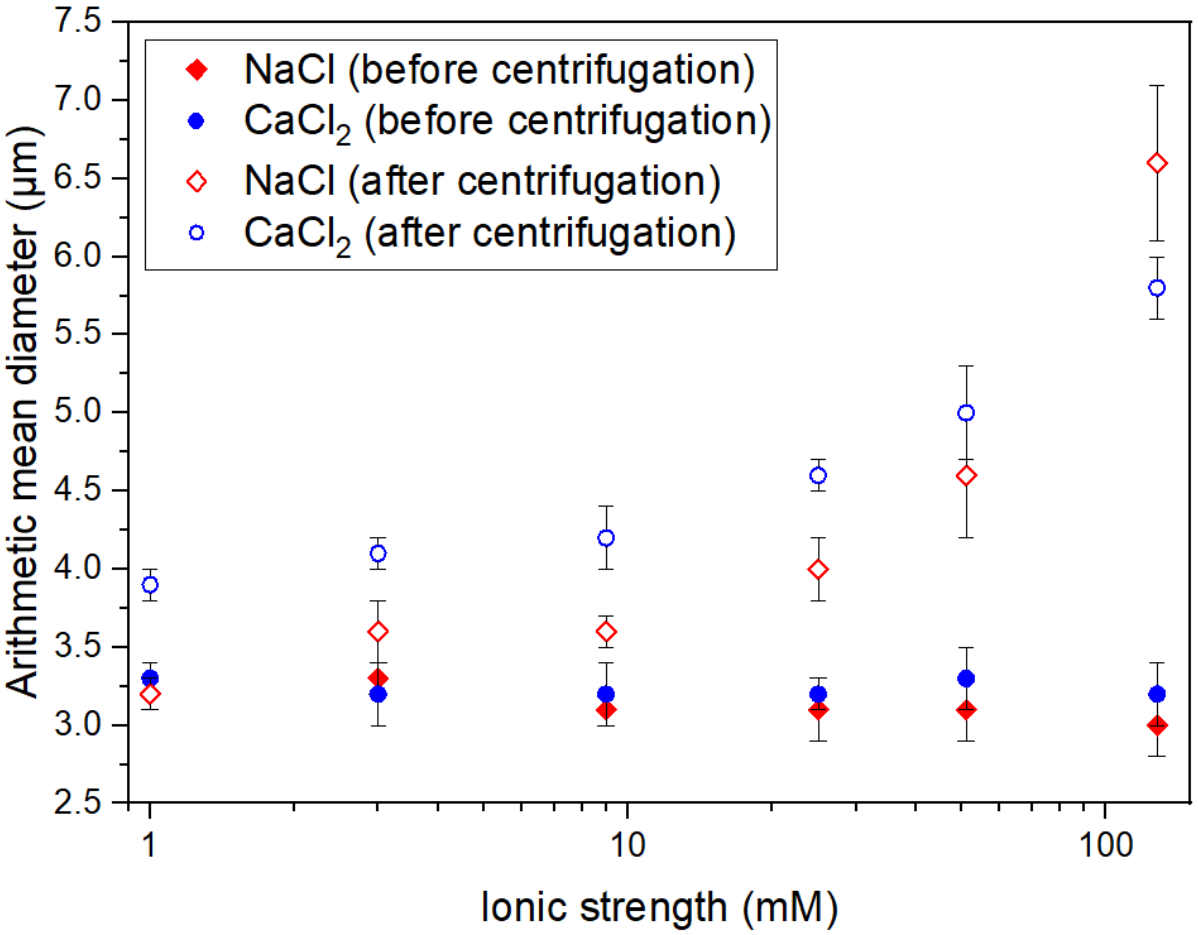

Figure 13: Arithmetic mean diameter of the largest droplets as a function of ionic strength before and after centrifugation process, at 20°C and 1 atm.

We note that the size of the elementary oil droplets in the production water before centrifugation is independent of the salinity of the brines used (mean diameter ≈ 3.1 µm) and in agreement with granulometry determinations. During centrifugation, the volume fraction of oil droplets at the top of the sample gradually increases to a concentrated oil droplet regime. In this regime, the effect of the salt promotes coalescence by reducing the electrostatic repulsion between the oil droplets and allowing the droplets to come closer, leading to an increase in the average diameter of the oil droplets. This effect is all the more marked as the ionic strength of the brines increases.

As mentioned above, the drops are all flocculated in the cream. In order to know if the flocculation is irreversible, the cream must be diluted and analyzed with granulometry. Unfortunately, the cream volume was too small to be able to carry out this measurement.

In conclusion, the effect of salts in PW subjected to centrifugation is to promote the coalescence in concentrated regime. In order to confirm the hypotheses on the effects of salts in PW, the critical force leading to coalescence was studied and the results obtained are presented in the following section.

ii. Critical force determination

One method used to characterize the coalescence of crude oil droplets was to measure the critical force required to form a macroscopic oil film at the top of synthetic PW. As presented in the Experimental section, the synthetic PWs were subjected to centrifugation and then the concentrated oil droplet phase (after the PW creaming) was observed under an optical microscope. The results of these centrifugation tests are reported in Table 2 (for NaCl) and Table 3 (for $CaCl_2$). In the tables, W indicates that the concentrated phase is still an emulsion (blue boxes) and O that an oil layer is observed, meaning that oil drops have coalesced (brown boxes). The experiments were repeated twice, and the applied osmotic pressures were calculated using the equation 7.

Table 2: Centrifugal force applied for 1 hour to synthetic PW as a function of ionic strength of NaCl brine.

	Centrifugal force (g) / Critical osmotic pressure (Pa)					
I (mM)	480g / 48 Pa	6310 g/ 632 Pa	11470 g/ 1152 Pa	17200 g/ 1728 Pa	24300 g/ 2440 Pa	29000 g/ 2913 Pa
1	W	W	W	W	W	O
3	W	W	O	O	O	O
9	W	W	O	O	O	O
26	W	W	O	O	O	O
51	W	O	O	O	O	O
128	W	O	O	O	O	O

Table 3: Centrifugal force applied for 1 hour to synthetic PW as a function of ionic strength of $CaCl_2$ brine.

	Centrifugal force (g) / Critical osmotic pressure (Pa)					
I (mM)	480g/ 48 Pa	6310 g/ 632 Pa	11470 g/ 1152 Pa	17200 g/ 1728 Pa	24300 g/ 2440 Pa	29000 g/ 2913 Pa
1	W	W	W	W	W	O
3	W	W	W	W	O	O
9	W	W	O	O	O	O
26	W	W	O	O	O	O
51	W	W	O	O	O	O
128	W	O	O	O	O	O

The purpose of this method is to determine the force required to overcome the electrostatic barrier and form a macroscopic oil film as a function of the ionic strength of the PW. We find that a high centrifugal force allows the formation of macroscopic oil films even at low salinity.

The results show that at low centrifugation speeds, the salts have little impact on coalescence and the emulsion remains stable. Above a certain centrifugal force, depending on ionic strength, the creamed emulsion undergoes coalescence. This means that the energy supplied by the centrifuge is sufficient to overcome the electrostatic barrier and thus allow the coalescence of the oil droplets. This barrier is reduced by the presence of salt in the production water. The osmotic pressure above which coalescence is observed is called “critical osmotic pressure”. We have observed that despite the formation of a macroscopic oil film after centrifugation, there are still oil droplets in water. It means that the centrifugation force applied is not sufficient to allow a complete coalescence of oil droplets.

There is a small difference between the influence of NaCl and $CaCl_2$ at a given ionic strength: emulsion stability tends to be better in the presence of $CaCl_2$. We have seen the same trend in the experiments conducted with the LUMiSizer. This could arise from a higher surface charge in the presence of $CaCl_2$ due to the nature of adsorbed crude's native acids. The accuracy on zeta potential determinations is unfortunately not sufficient to confirm this assumption.

The impact of salts on the critical osmotic pressure of oil droplets is presented in Figure 14. We find that the critical osmotic pressure decreases as the ionic strength of the brines increases. This means that salts reduce the resistance of the oil droplets to coalescence.

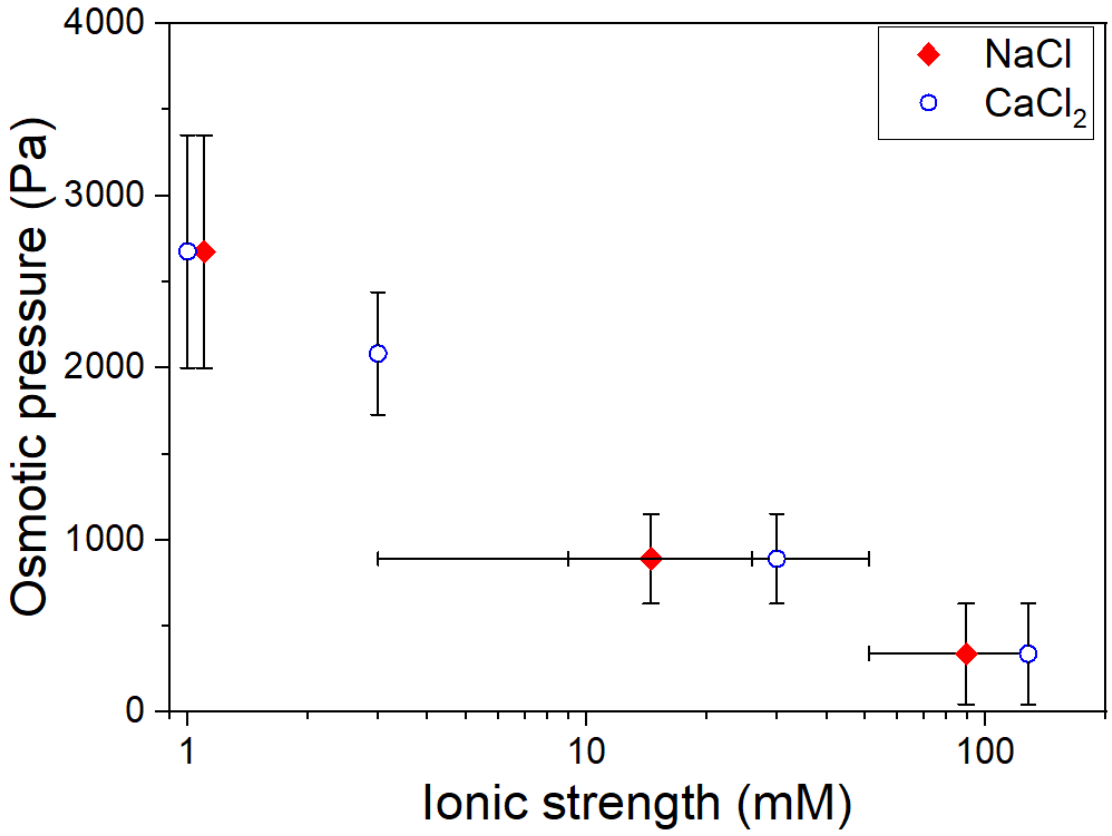

Figure 14: Critical osmotic pressure of the oil droplets as a function of the ionic strength of the NaCl and $CaCl_2$ solutions.

Note that the critical pressures do not seem to be very high. Tcholakova et al. observed that destabilization of emulsions stabilized by surfactants and proteins generally occurs in a pressure range from 20 to 100 kPa for droplets with a radius between 1 µm and 5 µm [47]. Here, the emulsions are therefore not strongly stabilized by the natural surfactants in the oil. It is well known that the stability of crude oil emulsions increases significantly with time, due to the development of interfacial elastic moduli over times of the order of a day [33]. The concentrated emulsions were used several days after their preparation and were very stable. However, their dilution with brine was made just prior to the centrifugation experiments. Because dilution with brines creates a new repartition of the oil surface-active species at the droplet's surface, the new surface layer is not yet consolidated, possibly explaining why the critical osmotic pressures are small. Prior equilibration of the PWs cannot be performed because it would require times comparable to creaming times, during which coalescence could occur,

biasing the determination of the critical osmotic pressure in the centrifugation experiments performed afterwards.

In conclusion, the effect of salts is to promote the coalescence under centrifugation in the concentrated regime. Flocculation is confirmed by the presence of flocs before centrifugation even if the flocs are formed by only a few droplets. Coalescence causes an increase in oil droplet size and the formation of a macroscopic oil film when sufficient centrifugal force is applied. These phenomena are due to the decrease in electrostatic repulsion between the oil droplets when the ionic strenght is increased.

c. The effect of the residual surfactant could have possibly played a role. Indeed, interfacial tension measurements showed that it was still present in the surface layers. However, this surfactant is nonionic and could not affect the electrostatic interactions between drops. Furthermore, the experiments of coalescence between drops and a planar oil-water interface discussed afterwards show the same correlations with the electrostatic interactions, despite there is no residual surfactant in these systems.Coalescence between oil drops and a planar oil-water interface

In order to investigate further the coalescence process, we measured the rupture time between a diluted crude oil drop of millimetric size and a planar diluted crude oil/brine interface using the protocol mentioned in the Experimental section. These measurements were performed with a diluted crude oil having an oil fraction of 90 wt% and brines containing either NaCl or $CaCl_2$ with different ionic strengths.

The images were video-recorded and evidenced different steps: 1) Formation of the drop; 2) Ascension of the drop; 3) Contact between the interface and the drop; 4) Drainage of the aqueous thin film; 5) Rupture of the aqueous thin film; 6) Complete coalescence of the drop at the water/oil interface. Figure 15 shows an example.

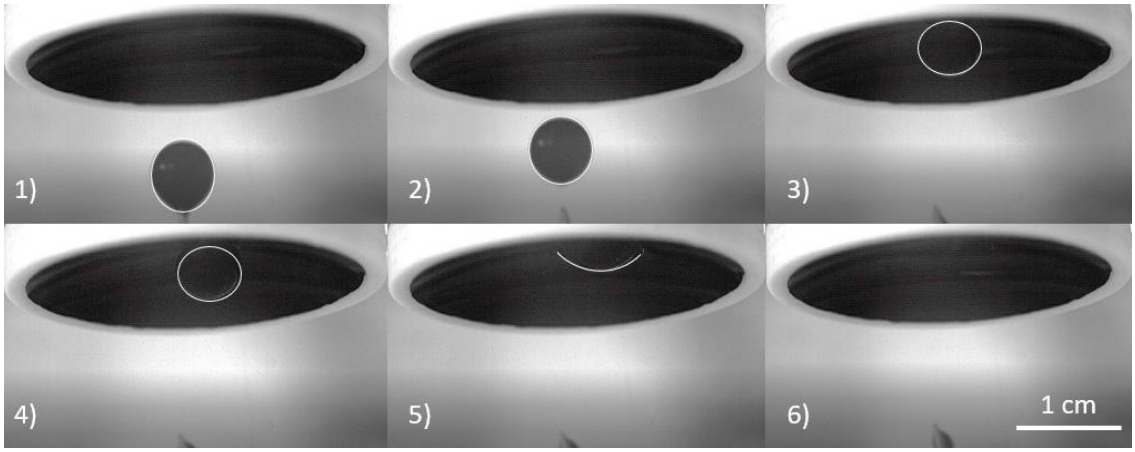

Figure 15: Images of the different steps of the coalescence process of a drop of oil diluted in xylene with a water/oil interface. The aqueous medium contains 7.5 g/L in NaCl. 1) Formation of the drop; 2) Ascension of

the drop; 3) Contact between the interface and the drop; 4) Drainage of the aqueous thin film; 5) Rupture of the aqueous thin film and spreading of the drop; 6) End of drop spreading. Scale = 1 cm.

The rising velocity is determined by the elapsed time between the detachment of the drop from the needle and the first "contact" between the drop and the water-oil interface. The spreading corresponds to the time elapsed between the rupture of the aqueous thin film and the end of the spreading of the drop on the water-oil interface. The rising velocities of the oil drops (about 5 cm/s) and the spreading time (about 0.65 s) are independent of the ionic strength of the brines in the range studied.

The rupture times are counted from the first "contact" between the drop and the water-oil interface and the rupture of the aqueous thin film. They are reported in Figure 16.

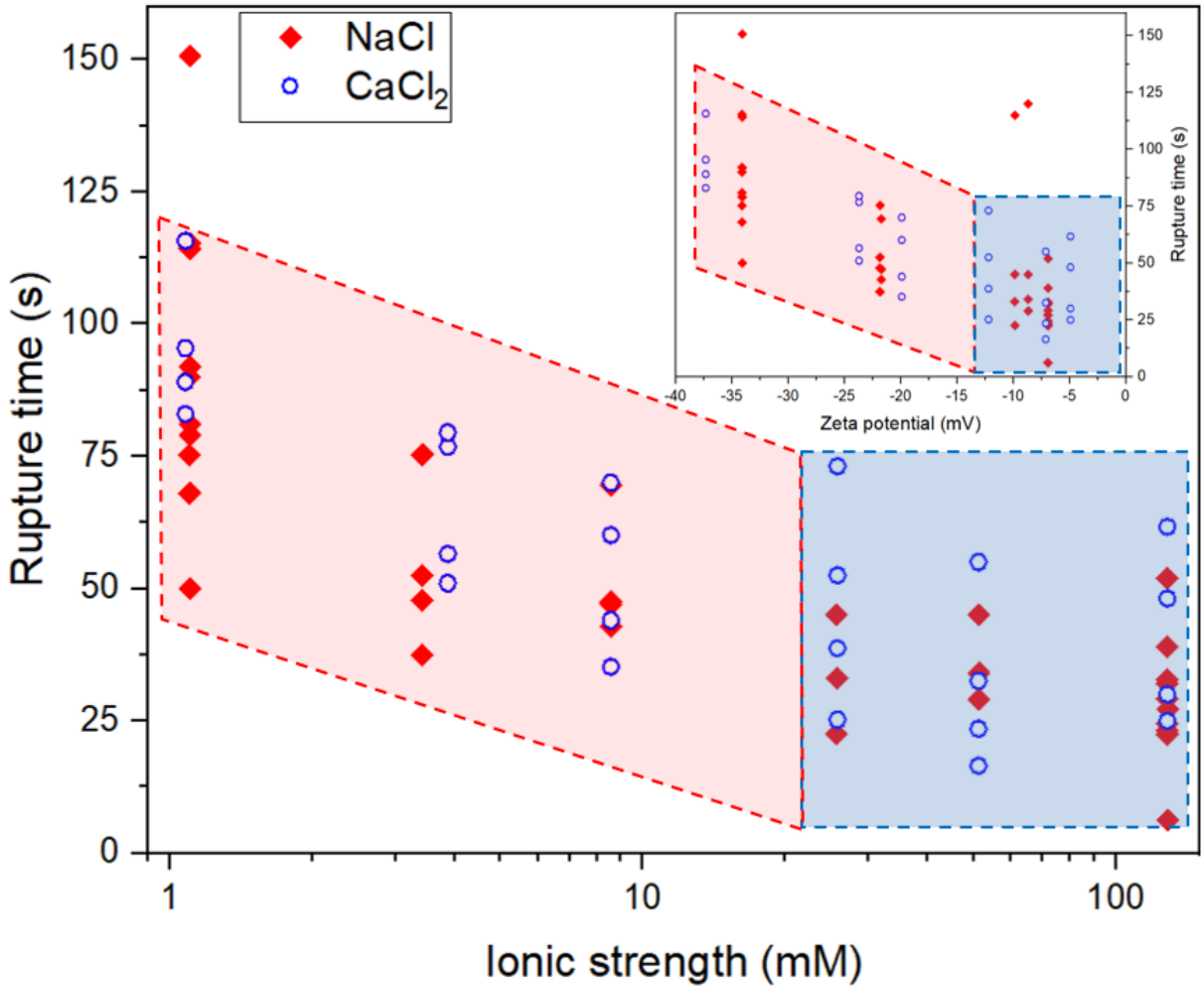

Figure 16: Rupture time of a drop of crude oil diluted 90 wt% in xylene as a function of the ionic strength and the zeta potential of the synthetic PW at different salinities with NaCl (red diamonds) and $CaCl_2$ (empty blue circles). Inserted image corresponds to the variation of the rupture time in function of the magnitude of the Zeta potential.

The rupture time decreases as the ionic strength of the brines increases; this phenomenon is likely due to the decrease of electrostatic repulsion between the interfaces. To verify this hypothesis, the rupture times as a function of the ZP of the PW are also shown in Figure 16. It should be noted that the increase in salinity in the concentration range studied does not significantly modify the density and the viscosity of the aqueous phase, therefore the effects of the salts observed are mainly interfacial effects.

These results show that for both the monovalent and the divalent salt (NaCl and $CaCl_2$), the rupture times decrease when the absolute values of ZP (which are related to the ionic strength) decrease.

Above an ionic strength of 50 mM, the ZP drops below 15 mV in absolute value and the rupture time remains rather constant. This is likely because the electrostatic potential barrier has been sufficiently screened. Chakibi et al. measured the rupture times of an aqueous thin film between a millimetric drop of crude oil in brine (NaCl) and an air/brine interface [20]. They observed that the rupture time also decreases as the ionic strength of the brines increases, this decrease is consistent with ZP measurements that support the hypothesis that electrostatic repulsion between the interfaces is reduced in the presence of salt in the PW. There is a good correlation between the measured rupture times in an oil/brine/oil and oil/brine/air system.

Wang et al. showed recently that salts in the aqueous phase delay the coalescence of toluene drops (stabilized by stearic acid) in brine, but in these experiments, the zeta potential should remain the same. They also found that the cation has no influence on the coalescence of toluene droplets [37]. The difference between our results and those of Wang et al. are due to the presence of oil indigenous surfactants at the droplets' surface, which solubility in brine depends on the concentration and nature of ions in brine. Coalescence of crude oil droplets cannot therefore be modeled with pure oils such as toluene.

Conclusion

In this paper, the impact of electrolytes on the stability of synthetic produced water was studied with different techniques using emulsions and macroscopic droplets. There is a good correlation between the results obtained at the macroscopic and microscopic scales.

It has been found that salts promote flocculation in a diluted oil droplet regime (before creaming) and coalescence in a concentrated regime under centrifugation (after creaming). The main cause of these phenomena is the reduction of electrostatic repulsion between the water/oil interfaces. This hypothesis has been verified by ZP measurements. The impact of salts on electrostatic repulsion is not only a screening effect of surface charges (decrease in the range of electrostatic interactions characterized by the Debye length), but the modification of the distribution of natural surfactants in the oil between the oily and aqueous phases, and the interface. Due to these modifications, the salts in solution reduce the surface charge of the oil droplets.

The reduction of electrostatic repulsion allows the droplets to come closer, leading to their flocculation and to the acceleration of the rupture of the aqueous thin film. The centrifugation experiments have shown that salts reduce the electrostatic barrier to be overcome to form a macroscopic oil film through the coalescence of oil droplets. Note that changes in interfacial composition can affect the rheology of the interfacial films which also controls coalescence. Disentangling the effects of zeta potential, ionic strength and interfacial rheology is not straightforward and will require further investigations.

IV. Appendix

Appendix 1 presents optical microscopy images of the PW creams obtained after one hour of centrifugation.

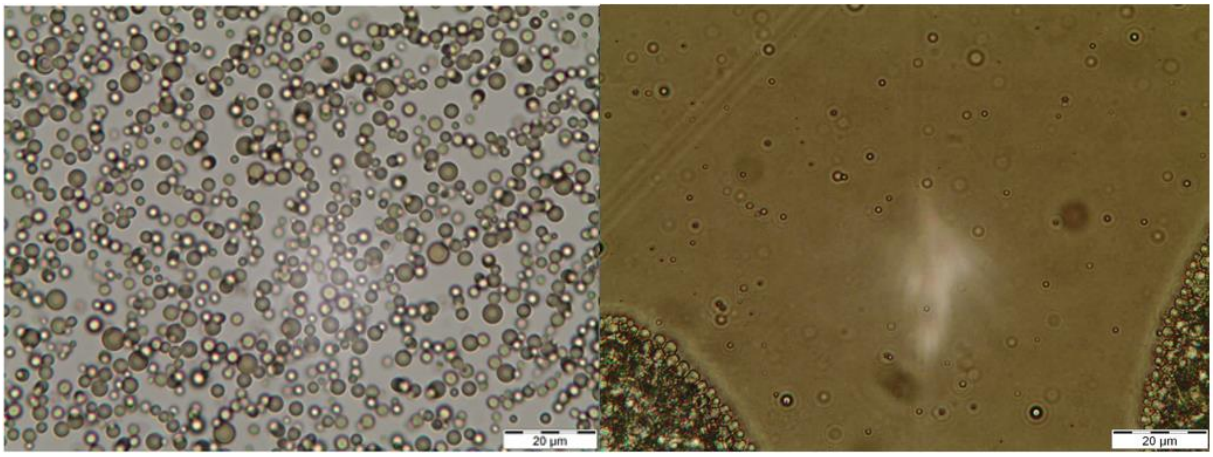

Appendix 1: Optical microscope images of the creams that form after centrifugation of the production water containing 0.5 wt% diluted oil; stable emulsion (left; the emulsion was partially diluted) and onset of coalescence revealed by the appearance of a macroscopic oil film (right). Scale bar = 20 µm.

In the following, we will describe the calculation of the critical osmotic pressure.

Above a critical rotation speed in the centrifuge, oil droplets begin to coalesce and form a macroscopic oil layer. The critical speed depends on the characteristics of the centrifuge (volume and shape of the bowl, inclination, distance from the axis) and is not an intrinsic property of the emulsion. It is therefore preferable to give the results in terms of critical osmotic pressure.

The centrifugal force is balanced by the osmotic pressure gradient [50].

$$\frac{d\Pi(r)}{dr} = -\Delta\rho \times r \times \omega^2 \times \Phi(r) \qquad \textbf{(A1)}$$

In this equation, r corresponds to the distance between the measuring point and the rotation axis, $\Pi(r)$ to the osmotic pressure, $\Delta\rho$ to the density difference between oil and water phases, ω to the rotation speed and $\phi(r)$ to the volume fraction of droplets.

If $r \geq r_2$ (see Appendix 2), there are no more oil droplets in the aqueous phase, then the osmotic pressure $\Pi(r_2)$ is equal to zero, as well as $\Phi(r_2)$. In the cream, $r_1 < r < r_2$, the pressure is large and ϕ is close to 1. Equation A1 can then be easily integrated, and we find the following relationship.

$$\Pi(r_1) - \Pi(r_2) = \Pi(r_1) = \Delta\rho \times \omega^2 \times \frac{(r_2^2 - r_1^2)}{2} \qquad \textbf{(A2)}$$

Here, r_1 and r_2 are the distances to the axis of the air-emulsion and emulsion-water interfaces respectively. Appendix 2 shows the position of the liquid container in the centrifuge.

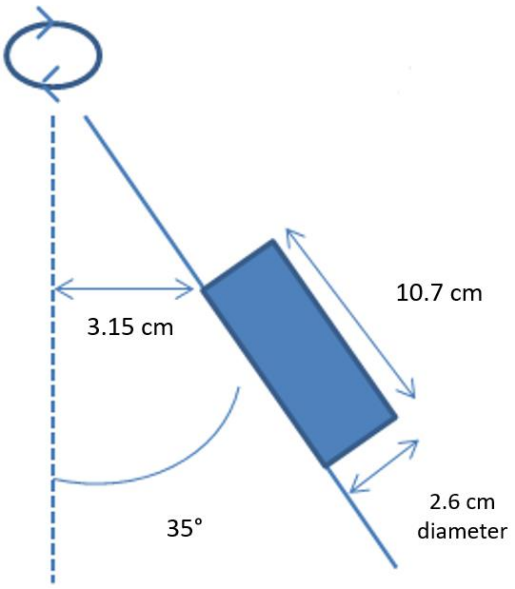

Appendix 2: Representation of the position of the centrifuge tube in the centrifugal.

Appendix 3 shows the creamed concentrated emulsion, represented by a thin red layer at the surface of the liquid (in blue). The emulsion layer is parallel to the axis of rotation. Since there are no more oil droplets in the blue region, the osmotic pressure is equal to zero for distances from the axis of rotation $r \geq r_2$. It is maximum for $r = r_1$. Appendix 3 shows the position of the emulsion during centrifugation.

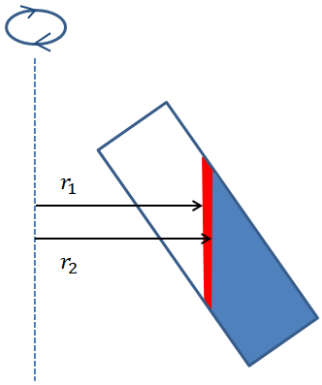

Appendix 3: Representation of oil layer (in red) and the aqueous phase (in blue) during centrifugation.

As the volume of oil is very small, we find from equation A3.

$$\Pi(r_1) \sim \Delta\rho \times \omega^2 \times r_1 \times \Delta r \text{ with } \Delta r = r_2 - r_1 \qquad \textbf{(A3)}$$

The volume available in the tube is 56.8 cm^3, which is more than the 40 cm^3 of liquid that was used for each test. At rest, when the tube is upright, the height of the liquid L is 7.5 cm. In rotation, the oil rises on the side to a height of 9.4 cm. This is less than the height of the tube (10.7 cm), as represented in Appendix 3. The distance r_1 from the axis of rotation is about 6.3 cm. The volume of cream is 0.22 cm^3 for 40 cm^3 of the sample. The centrifuged cream is a cylinder of height Δr and elliptical section of volume:

$$V = \frac{\Delta r \times \pi \times a^2}{\sin 35} \qquad \textbf{(A4)}$$

a being the tube radius. This gives a Δr of $1.96.10^{-4}$ m, i.e. about 0.20 mm.

In these centrifugation trials, osmotic equilibrium must be reached in order to determine the critical osmotic pressure. The oil droplet concentrated phase of the emulsions is observed with an optical microscope after centrifugation, i.e. one-hour waiting time. Sonneville-Aubrun et al. waited about 10 hours with their emulsions [48]. In our work, the cream layer is very thin (Δr= 0.20 mm), of the order of capillary length (l_{cap}= 0.21 mm for g^*= 480g, i.e. the lowest rotation of this work), so the oil droplet fraction should not change. The capillary length is calculated from the following relation:

$$l_{cap} = \sqrt{\frac{\gamma}{\Delta\rho \times g^*}} \qquad \textbf{(A5)}$$

In this equation, γ is the interfacial tension between the phases (in N/m), $\Delta\rho$ is the density difference between the phases (in kg/m^3) and g^* is the applied gravity (m/s^2).

References

(1) J.-L. Duplan; L. Nabzar. Water in fuel production: Oil production and refining. *IFP Energies Nouvelles* **2011**, 1–20.

(2) Hansen, B. R.; Davies, S. R. H. Review of potential technologies for the removal of dissolved components from produced water. *Chemical Engineering Research and Design,* 1994, 176–188.

(3) Dudek, M.; Kancir, E.; Øye, G. Influence of the Crude Oil and Water Compositions on the Quality of Synthetic Produced Water. *Energy Fuels* **2017**, *31* (4), 3708–3716. DOI: 10.1021/acs.energyfuels.6b03297.

(4) Das, P. C. Selection of Technology for Produced Water Treatment. *SPE Journal* **2012**, 1122–1128. DOI: 10.2118/151864-MS.

(5) Knudsen, B. L.; Hjelsvold, M.; Frost, T. K.; Svarstad, M.; Grini, P. G.; Willumsen, C. F.; Torvik, H. Meeting the Zero Discharge Challenge for Produced Water. *SPE Journal* **2004**, 71–73. DOI: 10.2118/86671-MS.

(6) Puprasert, C.; Hebrard, G.; Lopez, L.; Aurelle, Y. Potential of using Hydrocyclone and Hydrocyclone equipped with Grit pot as a pre-treatment in run-off water treatment. *Chemical Engineering and Processing: Process Intensification* **2004**, *43* (1), 67–83. DOI: 10.1016/S0255-2701(02)00154-X.

(7) Fakhru'l-Razi, A.; Pendashteh, A.; Abdullah, L. C.; Biak, D. R. A.; Madaeni, S. S.; Abidin, Z. Z. Review of technologies for oil and gas produced water treatment. *Journal of hazardous materials* **2009**, *170* (2-3), 530–551. DOI: 10.1016/j.jhazmat.2009.05.044.

(8) Weschenfelder, S. E.; Louvisse, A. M.; Borges, C. P.; Meabe, E.; Izquierdo, J.; Campos, J. C. Evaluation of ceramic membranes for oilfield produced water treatment aiming reinjection in offshore units. *Journal of Petroleum Science and Engineering* **2015**, *131*, 51–57. DOI: 10.1016/j.petrol.2015.04.019.

(9) Hemmingsen, P. V.; Silset, A.; Hannisdal, A.; Sjöblom, J. Emulsions of Heavy Crude Oils. I: Influence of Viscosity, Temperature, and Dilution. *Journal of Dispersion Science and Technology* **2005**, *26* (5), 615–627. DOI: 10.1081/DIS-200057671.

(10) Silset, A.; Flåten, G. R.; Helness, H.; Melin, E.; Øye, G.; Sjöblom, J. A Multivariate Analysis on the Influence of Indigenous Crude Oil Components on the Quality of Produced Water. Comparison Between Bench and Rig Scale Experiments. *Journal of Dispersion Science and Technology* **2010**, *31* (3), 392–408. DOI: 10.1080/01932690903110400.

(11) Ken Arnold; Maurice I. Stewart. *Surface Production Operations: Design of Oil-Handling Systems and Facilities*; Elsevier, 1999. DOI: 10.1016/B978-0-88415-821-9.X5000-3.

(12) Langevin, D. On the rupture of thin films made from aqueous surfactant solutions. *Advances in Colloid and Interface Science* **2020**, *275*, 102075. DOI: 10.1016/j.cis.2019.102075.

(13) Tambe, D. E.; Sharma, M. M. The effect of colloidal particles on fluid-fluid interfacial properties and emulsion stability. *Advances in Colloid and Interface Science* **1994**, *52*, 1–63. DOI: 10.1016/0001-8686(94)80039-1.

(14) Bresciani, A. E.; Alves, R. M. B.; Nascimento, C. A. O. Coalescence of Water Droplets in Crude Oil Emulsions:Analytical Solution. *Chem. Eng. Technol.* **2010**, *33* (2), 237–243. DOI: 10.1002/ceat.200900234.

(15) Sztukowski, D. M.; Yarranton, H. W. Oilfield solids and water-in-oil emulsion stability. *Journal of colloid and interface science* **2005**, *285* (2), 821–833. DOI: 10.1016/j.jcis.2004.12.029.

(16) Poteau, S.; Argillier, J.-F.; Langevin, D.; Pincet, F.; Perez, E. Influence of pH on Stability and Dynamic Properties of Asphaltenes and Other Amphiphilic Molecules at the Oil−Water Interface †. *Energy Fuels* **2005**, *19* (4), 1337–1341. DOI: 10.1021/ef0497560.

(17) Ata, S.; Pugh, R. J.; Jameson, G. J. The influence of interfacial ageing and temperature on the coalescence of oil droplets in water. *Colloids and Surfaces A: Physicochemical and Engineering Aspects* **2011**, *374* (1-3), 96–101. DOI: 10.1016/j.colsurfa.2010.11.012.
(18) Ayirala, S. C.; Yousef, A. A.; Li, Z.; Xu, Z. Coalescence of Crude Oil Droplets in Brine Systems: Effect of Individual Electrolytes. *Energy Fuels* **2018**, *32* (5), 5763–5771. DOI: 10.1021/acs.energyfuels.8b00309.
(19) PERU, D. A.; LORENZ, P. B. THE EFFECT OF EQUILIBRATION TIME AND TEMPERATURE ON DROP-DROP COALESCENCE OF WILMINGTON CRUDE OIL IN A WEAKLY ALKALINE BRINE. *Chemical Engineering Communications* **1989**, *77* (1), 91–114. DOI: 10.1080/00986448908940174.
(20) Chakibi, H.; Hénaut, I.; Salonen, A.; Langevin, D.; Argillier, J.-F. Role of Bubble–Drop Interactions and Salt Addition in Flotation Performance. *Energy Fuels* **2018**, *32* (3), 4049–4056. DOI: 10.1021/acs.energyfuels.7b04053.
(21) Arla, D.; Sinquin, A.; Palermo, T.; Hurtevent, C.; Graciaa, A.; Dicharry, C. Influence of pH and Water Content on the Type and Stability of Acidic Crude Oil Emulsions †. *Energy Fuels* **2007**, *21* (3), 1337–1342. DOI: 10.1021/ef060376j.
(22) Fakher, S.; Ahdaya, M.; Elturki, M.; Imqam, A. Critical review of asphaltene properties and factors impacting its stability in crude oil. *J Petrol Explor Prod Technol* **2020**, *10* (3), 1183–1200. DOI: 10.1007/s13202-019-00811-5.
(23) Langevin, D.; Argillier, J.-F. Interfacial behavior of asphaltenes. *Advances in Colloid and Interface Science* **2016**, *233*, 83–93. DOI: 10.1016/j.cis.2015.10.005.
(24) Mullins, O. C. The Modified Yen Model †. *Energy Fuels* **2010**, *24* (4), 2179–2207. DOI: 10.1021/ef900975e.
(25) Speight, J. G. Petroleum Asphaltenes - Part 1: Asphaltenes, Resins and the Structure of Petroleum. *Oil & Gas Science and Technology - Rev. IFP* **2004**, *59* (5), 467–477. DOI: 10.2516/ogst:2004032.
(26) Speight, J. G. Petroleum Asphaltenes - Part 2:The Effect of Asphaltene and Resin Constituents on Recovery and Refining Processes. *Oil & Gas Science and Technology - Rev. IFP* **2004**, *59* (5), 479–488. DOI: 10.2516/ogst:2004033.
(27) Buckley, J. S.; Fan, T. G. Crude oil/brine interfacial tension. *Petrophysics* **2007**, *48* (3), 175–185. Published Online: https://www.onepetro.org/journal-paper/SPWLA-2007-v48n3a1.
(28) McLean, J. D.; Kilpatrick, P. K. Effects of Asphaltene Solvency on Stability of Water-in-Crude-Oil Emulsions. *Journal of colloid and interface science* **1997**, *189* (2), 242–253. DOI: 10.1006/jcis.1997.4807.
(29) Hutin, A.; Argillier, J.-F.; Langevin, D. Influence of pH on Oil-Water Interfacial Tension and Mass Transfer for Asphaltenes Model Oils. Comparison with Crude Oil Behavior. *Oil Gas Sci. Technol. – Rev. IFP Energies nouvelles* **2016**, *71* (4), 58. DOI: 10.2516/ogst/2016013.
(30) Trabelsi, S.; Hutin, A.; Argillier, J.-F.; Dalmazzone, C.; Bazin, B.; Langevin, D. Effect of Added Surfactants on the Dynamic Interfacial Tension Behaviour of Alkaline/Diluted Heavy Crude Oil System. *Oil Gas Sci. Technol. – Rev. IFP Energies nouvelles* **2012**, *67* (6), 963–968. DOI: 10.2516/ogst/2012033.
(31) Lashkarbolooki, M.; Ayatollahi, S.; Riazi, M. The Impacts of Aqueous Ions on Interfacial Tension and Wettability of an Asphaltenic–Acidic Crude Oil Reservoir during Smart Water Injection. *J. Chem. Eng. Data* **2014**, *59* (11), 3624–3634. DOI: 10.1021/je500730e.
(32) Ayirala, S. C.; Al-Saleh, S. H.; Al-Yousef, A. A. Microscopic scale interactions of water ions at crude oil/water interface and their impact on oil mobilization in advanced water flooding.

Journal of Petroleum Science and Engineering **2018**, *163*, 640–649. DOI: 10.1016/j.petrol.2017.09.054.
(33) Okasha, T. M.; Alshiwaish, A. Effect of Brine Salinity on Interfacial Tension in Arab-D Carbonate Reservoir, Saudi Arabia **2009**, 1–9. DOI: 10.2118/119600-MS.
(34) Vijapurapu, C. S.; Rao, D. N. Compositional effects of fluids on spreading, adhesion and wettability in porous media. *Colloids and Surfaces A: Physicochemical and Engineering Aspects* **2004**, *241* (1-3), 335–342. DOI: 10.1016/j.colsurfa.2004.04.024.
(35) Xu, W.; Ayirala, S. C.; Rao, D. N. Measurement of Surfactant-Induced Interfacial Interactions at Reservoir Conditions. *SPE Reservoir Evaluation & Engineering* **2008**, *11* (01), 83–94. DOI: 10.2118/96021-PA.
(36) Garcia-Olvera, G.; Reilly, T. M.; Lehmann, T. E.; Alvarado, V. Effects of asphaltenes and organic acids on crude oil-brine interfacial visco-elasticity and oil recovery in low-salinity waterflooding. *Fuel* **2016**, *185*, 151–163. DOI: 10.1016/j.fuel.2016.07.104.
(37) Wang, T.; Andersen, S. I.; Shapiro, A. Coalescence of oil droplets in microchannels under brine flow. *Colloids and Surfaces A: Physicochemical and Engineering Aspects* **2020**, *598*, 124864. DOI: 10.1016/j.colsurfa.2020.124864.
(38) Walstra, P.; Smulders, P. E. Modern Aspects of Emulsion Science:Chapter 2. Emulsion Formation. *Royal Society of Chemistry* **1998**, 56–99. DOI: 10.1039/9781847551474.
(39) A.K. Chesters. The modelling of coalescence processes in fluid-liquid dispersions : a review of current understanding. *Chemical Engineering Research and Design* **1991**, *69* (A4), 259–270.
(40) Ivanov, I. B.; Kralchevsky, P. A. Stability of emulsions under equilibrium and dynamic conditions. *Colloids and Surfaces A: Physicochemical and Engineering Aspects* **1997**, *128* (1-3), 155–175. DOI: 10.1016/S0927-7757(96)03903-9.
(41) Vakarelski, I. U.; Manica, R.; Tang, X.; O'Shea, S. J.; Stevens, G. W.; Grieser, F.; Dagastine, R. R.; Chan, D. Y. C. Dynamic interactions between microbubbles in water. *Proceedings of the National Academy of Sciences of the United States of America* **2010**, *107* (25), 11177–11182. DOI: 10.1073/pnas.1005937107.
(42) Politova, N. I.; Tcholakova, S.; Tsibranska, S.; Denkov, N. D.; Muelheims, K. Coalescence stability of water-in-oil drops:Effects of drop size and surfactant concentration. *Colloids and Surfaces A: Physicochemical and Engineering Aspects* **2017**, *531*, 32–39. DOI: 10.1016/j.colsurfa.2017.07.085.
(43) O.D. Velev, G.N. Constantinides, D.G. Avraam, A.C. Payatakes, R.P. Borwankar. Investigation of Thin Liquid Films of Small Diameters and High Capillary Pressures by a Miniaturized Cell. *Journal of colloid and interface science* **1995**, *175* (1), 68–76. DOI: 10.1006/jcis.1995.1430.
(44) Politova, N.; Tcholakova, S.; Denkov, N. D. Factors affecting the stability of water-oil-water emulsion films. *Colloids and Surfaces A: Physicochemical and Engineering Aspects* **2017**, *522*, 608–620. DOI: 10.1016/j.colsurfa.2017.03.055.
(45) Tcholakova, S.; Denkov, N. D.; Ivanov, I. B.; Campbell, B. Coalescence stability of emulsions containing globular milk proteins. *Advances in Colloid and Interface Science* **2006**, *123-126*, 259–293. DOI: 10.1016/j.cis.2006.05.021.
(46) D. Arla. Naphthenic acid gas hydrates: influence of the water/oil interface on the dispersant properties of an acid crude., Pau. https://www.theses.fr/2006PAUU3002 (accessed 2021-04-24).
(47) Tcholakova, S.; Denkov, N. D.; Lips, A. Comparison of solid particles, globular proteins and surfactants as emulsifiers. *Phys. Chem. Chem. Phys.* **2008**, *10* (12), 1608. DOI: 10.1039/b715933c.

(48) Sonneville-Aubrun, O.; Bergeron, V.; Gulik-Krzywicki, T.; Jönsson, B.; Wennerström, H.; Lindner, P.; Cabane, B. Surfactant Films in Biliquid Foams †. *Langmuir* **2000**, *16* (4), 1566–1579. DOI: 10.1021/la990599k.

TOC Graphic